Simulating the escape of entangled photons from the event horizon of black holes in nonuniform optical lattices

Chong Sheng [1,*] Chunyu Huang,[1] Runqiu Yang,[2] Yanxiao Gong,[1] Shining Zhu,[1] and Hui Liu[1,†]

[1]*National Laboratory of Solid State Microstructures and School of Physics, Collaborative Innovation Center of Advanced Microstructures, Nanjing University, Nanjing, Jiangsu 210093, China*

[2]*Center for Joint Quantum Studies and Department of Physics, School of Science, Tianjin University, Yaguan Road 135, Jinnan District, 300350 Tianjin, China*

(Received 12 November 2020; accepted 16 February 2021; published 5 March 2021)

We investigate quantum walks in a noninertial frame with a Rindler metric, emulated by a nonuniform optical lattice with varying site couplings whose metric is mathematically equivalent to that of a Schwarzschild black hole near the event horizon. The optical trapping of single photons and two indistinguishable photons in such nonuniform lattices conforms to a well-known classical physical recognition due to the strong gravitational force of black holes. Counterintuitively, there is an optical escape for path-entangled photons for which one photon is captured, while the other photon escapes. Intriguingly, we find that the counterintuitive phenomenon has a distinct escape mechanism compared to Hawking radiation, which is wholly due to quantum interference. Additionally, we investigate the entanglement decay for this maximally entangled state in the emulated noninertial frame. Our study paves the way for a tabletop platform for understanding quantum effects under general relativity.

DOI: 10.1103/PhysRevA.103.033703

I. INTRODUCTION

Since the beginning of the detection of gravitational wave [1,2] and the imaging of black holes [3], a broad interest has been stimulated in the study of black holes, and the Nobel Prize in physics has been awarded twice in the last 5 y to the research of black holes. However, determining how to establish a unified theory combining quantum mechanics and general relativity remains an open question. Additionally, the quantum effects of black holes, such as Hawking radiation [4] and Penrose super-radiance [5], have not been validated by experimental observation in astronomy since there has been a lack of good observation tools up to now. However, the quantum simulation [6–8], Feynman's innovative idea that one could employ a controllable quantum system to mimic other quantum systems, could dispose of these intractable problems with the quantum effects of black holes. One of the typical examples was the Hawking-Unruh [9] effect, which has been successfully emulated using a variety of quantum architectures ranging from ultracold atoms [10], Bose-Einstein condensates [11], trapped ions [12], and Fermi-degenerate liquids [13] to superconducting circuits [14] and nonlinear optical media [15–17]. In particular, with the flourishing of metamaterials [18,19] and transformation optics [20–22], some other phenomena for general relativity have been emulated, including the gravitational lensing of black holes [23–27] and cosmic strings [28,29], Einstein rings [30], wormholes [31–33], the "Big Bang" [34], and cosmological inflation [35]. Additionally, optical lattices have been among the most versatile platforms in manipulating photons. Optical lattices have also allowed for the simulation of quantum physics in curved space, such as fermion pair production [36,37] near the event horizons of black holes and in a time-dependent space-time, hyperbolic space [38,39] with constant negative curvature connecting to anti–de Sitter/conformal field theory correspondence. However, to the best of our knowledge, the direct use of quantum entangled photons in optical lattices to simulate quantum effects for black holes has not been reported yet.

Quantum walks (QWs) of correlated photons [40–44] in optical lattices have been used to exhibit nonclassical correlations as a result of uniquely quantum-mechanical behavior, in contrast to single-photon QWs that could be described with classical wave theory, and a large coherent superposition state that has given rise to an advantage in massive parallelism computing has been generated [45,46]. Additionally, QWs for multiple indistinguishable photons have also been exploited to simulate a variety of other quantum-dynamical processes such as excitation transfer across spin chains [47] and energy transport in photosynthetic complexes [48]. However, all these works about QWs were limited for uniform lattices, leaving the QWs of correlated photons in a nonuniform lattice rarely investigated.

In this work, we first propose and exploit QWs in nonuniform optical lattices to study entangled photons in the emulated noninertial frame with the Rindler metric, whose metric is mathematically equivalent to that of the event horizon of Schwarzschild black holes. Although an optical analog space-time is not a faithful representation of an actual space-time

*csheng@nju.edu.cn
†liuhui@nju.edu.cn

[49], some certain aspects of gravitating systems can be well preserved and emulated using such an analog space-time. Inspired by transformation optics mapping curved space to a nonuniform effective optical medium, we map the curved space to nonuniform lattices with a continuously changing coupling coefficient. In addition, the two-dimensional Rindler metric that describes an accelerated noninertial frame is achievable by deliberately tuning the coupling coefficient between identical waveguides with a linear relationship as a function of the waveguide sites. We investigate the accelerated walks of single photons for which the main lobes of the QWs have the exponential evolution decided by the acceleration of the frame. Interestingly, the waveguide decoupling from other waveguides in the nonuniform optical lattice acts as the event horizon site ($n = 0$). And the main lobe toward the event horizon site is dominant with the evolution. Moreover, we also explore the evolution of the photon-number correlation of two indistinguishable photons, which clearly exhibits the fact that the photons are bunched at the waveguide near the event horizon. And, this photon bunching in the nonuniform lattice is a good simulation of a photon being trapped by black holes, which is a well-known classical physical process, due to the strong gravitational force of a black hole. However, if we input two photons in a type of path-entangled NOON state, the photons have a probability of escaping from the event horizons of black holes. This phenomenon is completely contrary to the concept that photons are always captured by black holes, as predicted by classical physics. Additionally, we find that this type of photon escape has a totally distinct mechanism compared to that of Hawking radiation, whose mechanism is that particles with negative energy are captured by black holes while positive energy escapes. The escape for path-entangled photons is wholly due to the quantum interference. Moreover, the calculated entanglement entropy for this maximal entanglement state begins decaying, and it is a function of the acceleration of the noninertial frame, which conforms to the expectation with the Unruh effect [50,51].

This paper is organized as follows. In Sec. II, we make a brief view to map the 1+1-dimensional Rindler metric into one-dimensional waveguide lattices and obtain the Green function to depict quantum walks of photons in such a nonuniform lattice. In Sec. III, we investigate quantum walks of single photons and two indistinguishable photons. In Sec. IV, we investigate the quantum walks of path-entangled NOON photons in the emulated noninertial frame with a Rindler metric. Moreover, we also study the entanglement of such NOON photons in the nonuniform optical lattices. In Sec. V, we give a summary and some discussions.

II. THE GREEN FUNCTION NEAR THE EVENT HORIZON

The goal of this section is to obtain the Green function in the nonuniform optical lattices which emulate the noninertial frame with a Rindler metric. First, we map the 1+1-dimensional Rindler metric [50] into one-dimensional waveguide lattices, whose metric is as

$$ds^2 = -(\alpha x)^2 dt^2 + dx^2, \tag{1}$$

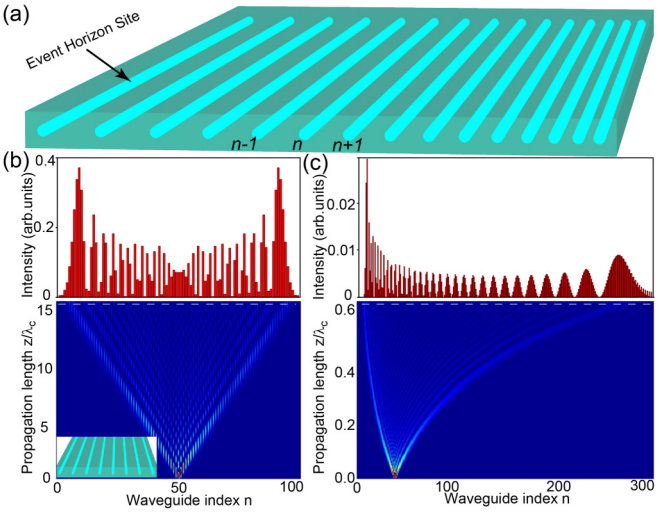

FIG. 1. Quantum walks of single photons in uniform and nonuniform optical lattices corresponding to the flat space and a noninertial frame with the Rindler metric. (a) Schematic of nonuniform lattices with coupling coefficient linearly depending on waveguide sites as $\kappa_{n,n+1} = \alpha n \kappa_0/2$. Here, α is the acceleration. (b) Quantum walks of single photons in uniform lattices. The inset is the output pattern for the white dashed line in the evolution picture. The site where single photons are injected is $n = 50$. (c) Quantum walks of single photons in nonuniform lattices, which emulate a noninertial frame with the Rindler metric. The inset is the output pattern for the white dashed line in the evolution picture. The site where single photons are injected is $n = 45$. Here, $\lambda_c = \pi/(2\kappa_0)$, where κ_0 is the coupling coefficient.

where α is the acceleration. Intriguingly, the Rindler metric is mathematically equivalent to the metric of Schwarzschild black hole near the event horizon after only considering the radial direction under the restriction $\alpha x \ll 1$ (see details in Appendix A). In this work, the analog of the event horizon of black holes is constructed inspired by transformation optics that is not a perfect simulator. Given that transformation optics preserved the coordinate description of light whereas at the expense of some other feature of the emulated gravitational system, we exploit the invariance between the emulated and actual space-time as a tool to study some fascinating gravitational phenomena due to lacking astronomical observational methods. And, the gravitational field is encoded into lattices of identical evanescently coupled waveguides, in which the propagation of photons is determined by two parameters: the propagation constant and the coupling constant between waveguides. According to the mapping relationship inspired by transformation optics, a lattice of an identical waveguide, in which the coupling constants have a linear relationship as a function of the waveguide site n [as shown in Fig. 1(a)], the photons propagating within can describe photons evolving in an accelerated noninertial frame (see details in Appendix A). To study the propagation of photons in these types of structures, we quantize the fields in the lattice. Since each of the waveguides supports a single mode, the field in waveguide n is represented by the bosonic creation and annihilation operators $a_n^\dagger$ and a_n, which satisfies the commutation relationships $[a_m a_n^\dagger] = \delta_{m,n}$. The operators evolve according to the

Heisenberg equations:

$$-i\frac{\partial a_n^\dagger}{\partial z} = \beta_0 a_n^\dagger + \frac{\alpha(n-1)\kappa_0}{2} a_{n-1}^\dagger + \frac{\alpha n \kappa_0}{2} a_{n+1}^\dagger. \quad (2)$$

Here, z is the spatial coordinate along the propagation axis, which plays the role of the time t for the waveguide evolution, and β_0 (κ_0) is the propagation (coupling) constant. The evolution of the creation and annihilation operators is calculated using the Green function $U_{m,n}(z)$ of the above equation, $a_m^\dagger(z) = \sum_n U_{m,n}(z) a_n^\dagger(z=0)$. The unitary transformation $U_{m,n}(z)$ describes the amplitude for the transition of a single photon from waveguide n to waveguide m. The Green function is given by (see details in Appendix B):

$$U_{m,n}(z) = \frac{1}{2\pi}\int_{-\pi}^{\pi} dq \exp\Big\{imq - i2n \arctan \times \Big[\tanh\Big(\operatorname{arctanh}\Big[\tan\frac{q}{2}\Big] - \frac{\alpha\kappa_0 z}{2}\Big)\Big] - i\beta_0 z\Big\}, \quad (3)$$

where the quasimomentum q is confined to the zone $-\pi \leqslant q \leqslant \pi$. In the following numerical calculations, the number of waveguide sites is limited and is about $m \approx 100$. Here we take the waveguide lattice in silicon on insulator as an example. To satisfy the assumption about the space near the event horizon, this restriction requires that the distance between waveguides $d \ll 1/\alpha\kappa_0 m = 10\ \mu$m with considering $\alpha = 1$, $\kappa_0 \approx 0.001\ \mu\text{m}^{-1}$. In fact, the distance between waveguides with submicrometer precision is easily achieved for the current (micro)-nanofabrication.

III. QUANTUM WALKS OF SINGLE PHOTONS AND TWO INDISTINGUISHABLE PHOTONS

Since any input state can be expressed with the creation operators $a_m^\dagger$ and the vacuum state $|0\rangle$, the quantum walks of photons in the emulated noninertial frame with a Rindler metric can be calculated using Eq. (3). The probability of being located at site m when a photon is injected into the lattice at site $n = n_0$ is given by the photon density $\rho_m = \langle a_m^\dagger a_m\rangle = |U_{m,n_0}|^2$, as depicted in Fig. 1(b). The photon exhibits an accelerated walk: it spreads across the lattice by tunneling between the waveguides in a pattern characterized by two peaks at the two edges of the distribution. Both contours of the two peaks have an exponential form that is dependent on the acceleration α, in contrast to two strong and linear "ballistic" lobes in the flat space [see the inset in Fig. 1(a)]. Interestingly, the left peak toward the event horizon site is dominant, whereas the right peak away from the event horizon site becomes weak with the longer propagation distance. We explain that from the perspective of the Green function. When the photons propagate in a large distance for $z \gg 2/(\alpha\kappa_0)$, the above equation can be simplified as $U_{m,n}(z) \cong \delta(m)\exp(\frac{in\pi}{2} - i\beta_0 z)$. Therefore, the photons are captured to the event horizon site no matter which sites a photon is injected into, as shown in Fig. 2. In addition, the trapping process of single photons is similar to that of photons being captured by a black hole. The similarity is also confirmed by the fact that the 1+1-dimensional Rindler metric is mathematically equivalent to that of a Schwarzschild black hole near the event horizon after only considering the radial direction.

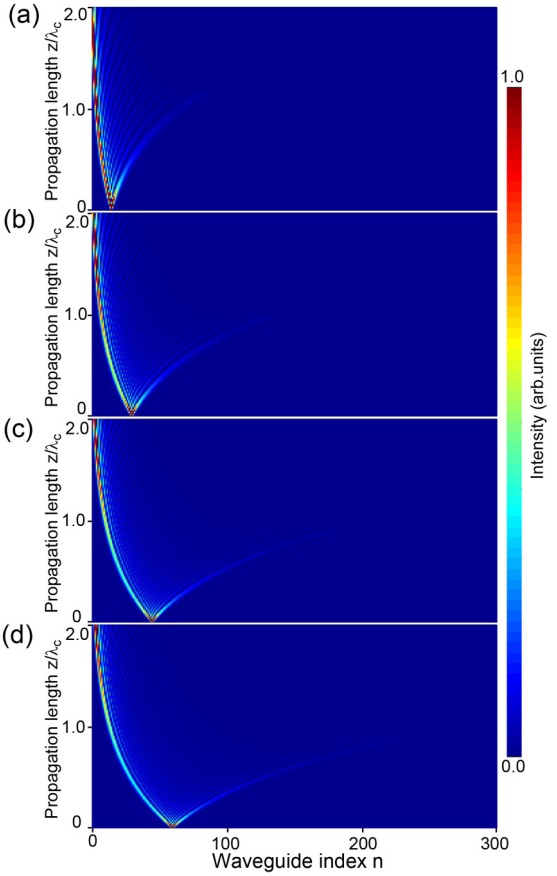

FIG. 2. The evolution of single photons in the emulated noninertial frame with different injection sites. In the calculation, the number of waveguide sites is 300, and the acceleration is $\alpha = 1$. In (a), the site of injecting photons is $n = 15$; in (b), the site of injecting photons is $n = 30$; in (c), the site of injecting photons is $n = 45$; in (d), the site of injecting photons is $n = 60$. Here, $\lambda_c = \pi/(2\kappa_0)$, where κ_0 is the coupling coefficient.

Furthermore, in order to study the quantum nature of photons in the emulated accelerated noninertial frame, we focus on the evolution of nonclassical features with the photon-number correlation function of $\Gamma_{m,n}^{(p,q)} = \frac{1}{q!p!}\langle a_m^{\dagger p} a_n^{\dagger q} a_n^q a_m^p\rangle$, which indicates the probability to detect p photons in waveguide site m and q photons in waveguide site n. For two indistinguishable input photons, the correlation is $\Gamma_{m,n}^{(1,1)} = \frac{1}{1+\delta_{m,n}}|U_{m,m'}U_{n,n'} + U_{n,m'}U_{m,n'}|^2$, where m' and n' are the sites that photons are injected into. As described below, we study the correlation $\Gamma_{m,n}^{(1,1)}$ for three distinct two-photon input states: (i) the two photons are coupled into a single waveguide [Fig. 3(a)]; (ii) the two photons are coupled into two adjacent waveguides [Fig. 3(b)]; and (iii) the two photons are coupled into waveguides separated by one waveguide [Fig. 3(c)]. Although the correlation patterns for the three cases are a little different, two photons have an ultrahigh probability to bunch near the event horizon site after a large enough propagation distance, indicating that two indistinguishable photons are trapped.

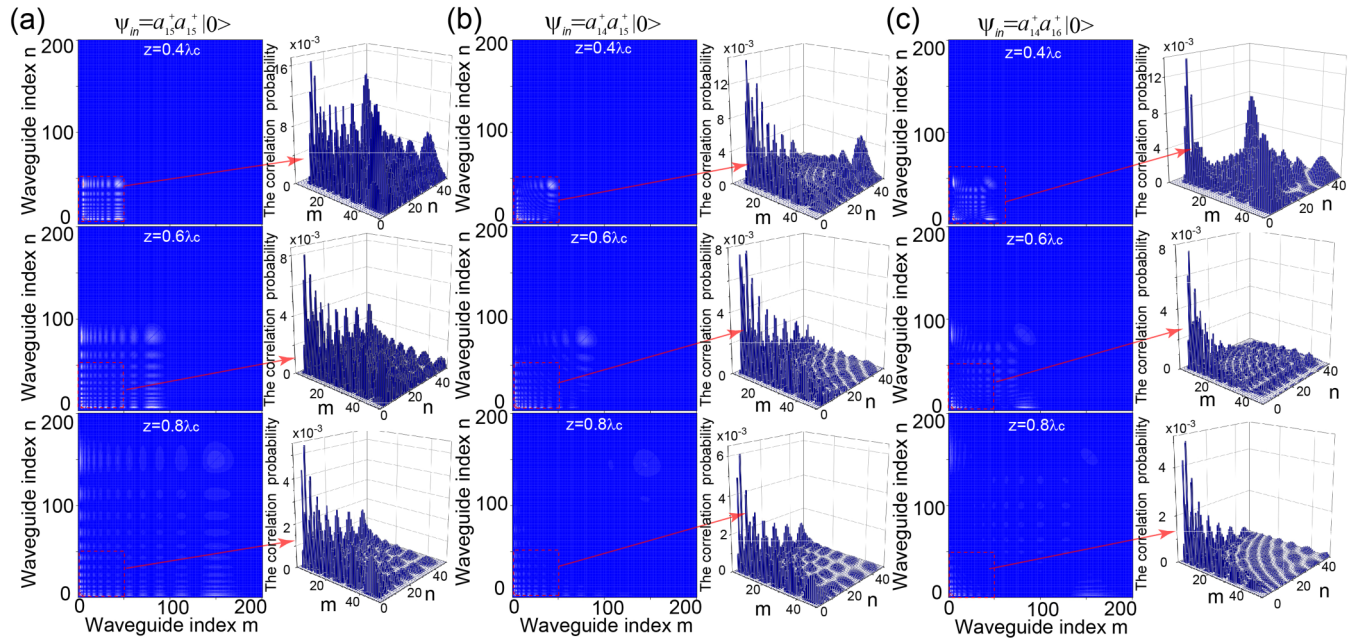

FIG. 3. Quantum walks of two input indistinguishable photons in the nonuniform lattice that emulate a noninertial frame. (a) The multiple detection probability $\Gamma_{m,n}^{(1,1)}$ at several propagation distances for which both photons are coupled into a single waveguide ($n_1 = n_2 = 15$). (b) The multiple detection probability $\Gamma_{m,n}^{(1,1)}$ at several propagation distances for which both photons are coupled into two adjacent waveguides ($n_1 = 14, n_2 = 15$). (c) The multiple detection probability $\Gamma_{m,n}^{(1,1)}$ at several propagation distances for which both photons are coupled into waveguides separated by one waveguide ($n_1 = 14, n_2 = 16$). Here, $\lambda_c = \pi/(2\kappa_0)$, where κ_0 is the coupling coefficient.

IV. QUANTUM WALKS OF PATH-ENTANGLED PHOTONS AND THE ENTANGLEMENT IN THE EMULATED NONINERTIAL FRAME

In addition to indistinguishable photons, what happens to the entangled photon pairs in the emulated accelerated noninertial frame is more attractive. The entanglement is a counterintuitive feature of quantum physics that is at the heart of quantum technology. In this work, we employ path-entangled NOON states with $N = 2$ injected into two adjacent waveguides $|\psi\rangle = \frac{1}{2}(a_m^{\dagger 2} + e^{-i\varphi}a_{m+1}^{\dagger 2})|0\rangle$ with a different phase φ. We also use the photon number correlation $\Gamma_{m,n}^{(1,1)}$, the probability of detecting one photon at waveguide m and another photon at waveguide n, to depict the nonclassical features of the NOON states. As described below, we investigate the correlation $\Gamma_{m,n}^{(1,1)}$ for three distinct NOON input states for $\varphi = \pi, \pi/2, 0$. For $\varphi = \pi$, the photons are bunching near event horizon waveguide site after enough propagation distance, as shown in Fig. 4(a), which conforms to the expectation that photons are trapped in the event horizon site. Additionally, for $\varphi = \pi/2$, although the two photons bunching near the event horizon site have quite a probability, there is also a probability that one photon is trapped near the event horizon site, and the other photon escapes [see Fig. 4(b)]. However, for $\varphi = 0$, one photon is captured in the event horizon site, and the other photon is definitely likely to escape, as shown in Fig. 4(c). The phenomena for the last two cases are totally contrary to the recognition that photons are always trapped by black holes. As mentioned above, the Rindler metric, mapped by the designed coupling waveguide lattices in this work, is mathematically equivalent to that of a Schwarzschild black hole near the event horizon. Our results clearly exhibit a phenomenon exists in which that one photon of such a NOON state ($|\psi\rangle = \frac{1}{2}(a_m^{\dagger 2} + a_{m+1}^{\dagger 2})|0\rangle$) is captured by the event horizon of a black hole and the other photon escapes. In addition, this photon escape is totally distinct from that caused by Hawking radiation, whose mechanism is that vacuum fluctuation generated positive and negative energy particle pairs, and the particles with negative energy are captured by black holes, whereas the particles with positive energy escape. In contrast, the photon escape for path-entangled photons is caused by quantum interference.

Furthermore, according to the Unruh effect [51], the entanglement is an observer-dependent quantity in noninertial frames, and the maximally entangled state becomes less entangled if the observers are in an accelerated frame. In this work, we inject this type of NOON state $|\psi\rangle = \frac{1}{2}(a_0^{\dagger 2} + a_1^{\dagger 2})|0\rangle$ between the event horizon waveguide site ($n = 0$) and its adjacent waveguide site ($n = 1$). Among the accelerated lattice, the event horizon waveguide is decoupled from other waveguides due to the coupling between the event horizon waveguide and its adjacent waveguide site is zero. Since the photons propagate in the event horizon site, the photons do not interact with the outside environment waveguide, which implies that the photons are in a still state. However, for the photons propagating near the event horizon waveguide site, the photons spread into the lattice in an accelerated fashion, and the lattice is viewed as an accelerated frame. A consequence of this effect is that an entangled pure state becomes degraded. Furthermore, we exploit the logarithmic negativity to determine the entanglement of such a NOON state evolving in the nonuniform lattices (see details in

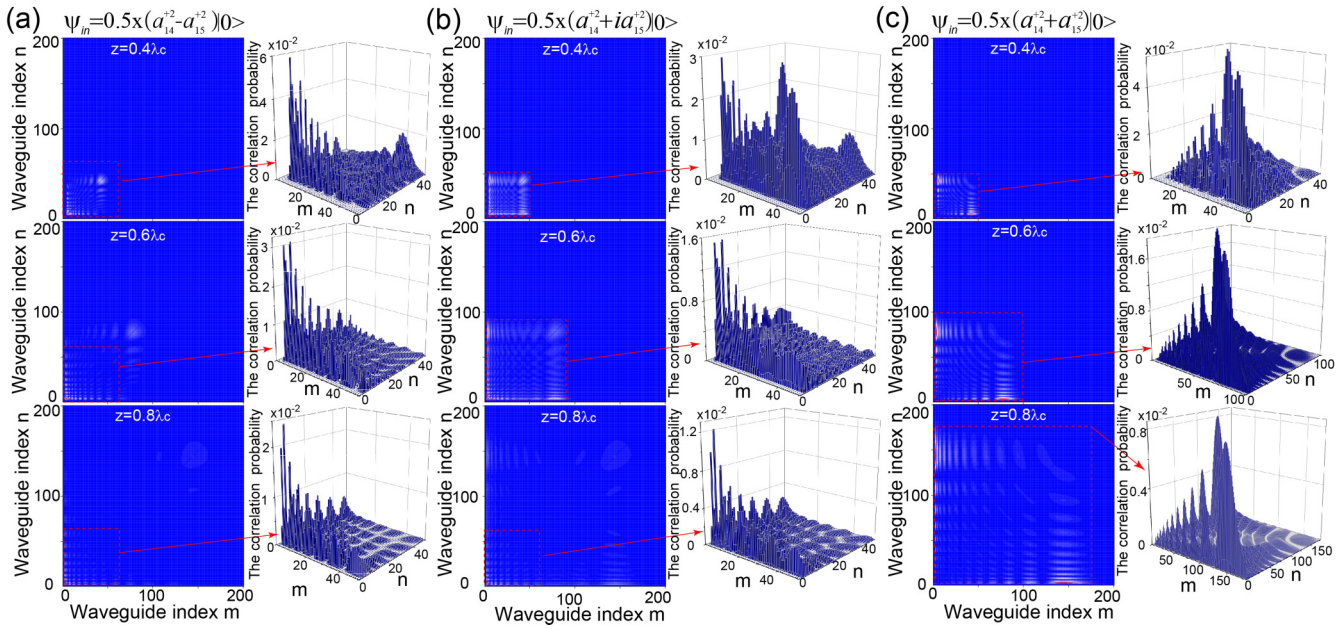

FIG. 4. Quantum walks of path-entangled NOON photons with $N = 2$ ($|\psi\rangle = \frac{1}{2}(a_m^{\dagger 2} + e^{-i\varphi}a_{m+1}^{\dagger 2})|0\rangle$) coupling to two adjacent waveguides with different phases φ in the nonuniform lattices that emulate a noninertial frame. Here, $m = 14$, $\lambda_c = \pi/(2\kappa_0)$, where κ_0 is the coupling coefficient. (a) The multiple detection probability $\Gamma_{m,n}^{(1,1)}$ at several propagation distances for $\varphi = \pi$. (b) The same as (a) for $\varphi = \pi/2$. (c) The same as (a) for $\varphi = 0$.

Appendix C). Figure 5(a) exhibits the entanglement entropy with distinct accelerations as a function of the propagation distance. At the initial time, the NOON state has a maximal entanglement entropy of $E_s = 1$. In addition, the entanglement entropy becomes degraded with the propagation and tends toward $E_s = 0$, which suggests that the state's distillable entanglement vanishes. Furthermore, the decaying rate of the entanglement entropy becomes faster with a larger acceleration. This phenomenon is more clearly illuminated in Fig. 5(b), which exhibits the entanglement entropy monotonically decreases with the increasing of the acceleration for the same propagation distance of the NOON state. Additionally, the relationship between the entanglement entropy and the acceleration conforms to the prediction for the Unruh effect that the entanglement is an observer-dependent quantity, and the maximally entangled state becomes degraded in an accelerated noninertial frame.

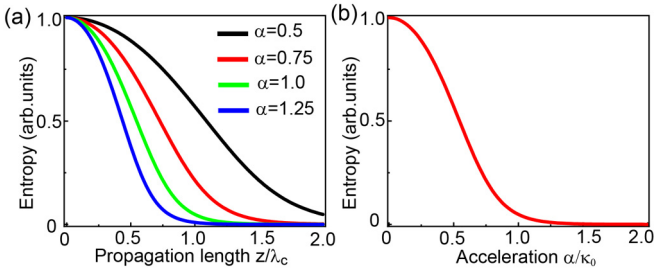

FIG. 5. Entanglement entropy in the nonuniform optical lattice that emulates a noninertial frame. (a) The relationship between the entanglement entropy and the propagation length for distinct accelerations. The different line colors represent different accelerations α. (b) The relationship between the entanglement entropy and the acceleration α for the same propagation length ($z = \lambda_c$). Here, $\lambda_c = \pi/(2\kappa_0)$, where κ_0 is the coupling coefficient.

V. CONCLUSION

In conclusion, we proposed and studied the quantum walks of single photons, correlated photons, and path-entangled photons in a noninertial frame with the Rindler metric. Additionally, the noninertial frame was emulated by lattices with identical waveguides that had a linear coupling coefficient that depended on sites inspired by transformation optics. Since the Rindler metric is identical to that of a Schwarzschild black hole near the event horizon when only considering the radial direction, we clearly observed the optical trapping of single photons and two indistinguishable photons in nonuniform optical lattices, which conformed to a well-known classical physical process due to the strong gravitational force of a black hole. Counterintuitively, we found that for the optical escape for path-entangled NOON states, one photon was captured, whereas another photon escaped. This phenomenon was contrary to the recognition that photons should always be captured by a black hole. Intriguingly, the counterintuitive phenomenon for path-entangled photons had a distinct escape mechanism compared to Hawking radiation. Furthermore, we investigated the entanglement decay for this maximally entangled state in the emulated noninertial frame, and the degeneracy was conformal to the prediction made using the Unruh effect. We believe that this investigation of entangled photons near the event horizon of black holes emulated by optical lattices will provide a platform for understanding quantum effects in the context of general relativity, and even the nature of quantum gravity. On the other hand, inspired by the concept in general relativity, we can design such

novelty optical devices to manipulate the classical and quantum property of photons, such as the omnidirectional absorber for photons inspiring by black holes and the entanglement manipulation in a noninertial frame.

ACKNOWLEDGMENTS

This work was financially supported by the National Key R&D Program of China (Grants No. 2017YFA0303702 and No. 2017YFA0205700), the National Natural Science Foundation of China (Grants No. 11690033, No. 61425018, No. 11621091, and No. 11704181), and the Fundamental Research Fund for the Central Universities, China (Grant No. 14380139).

APPENDIX A: THE MAPPING RELATION BETWEEN NONUNIFORM WAVEGUIDES LATTICES AND SPACE-TIME WITH RINDLER METRIC

We consider the line element of a two-dimensional Schwarzschild space-time with only radical direction ($d\theta = 0, d\varphi = 0$)

$$ds^2 = -(1 - r_s/r)dt^2 + (1 - r_s/r)^{-1}dr^2. \tag{A1}$$

Here r_s is the radius of the Schwarzschild black hole. When considering the space near the event horizon $r = r_s + \rho^2/4r_s$ and $0 < \rho \ll r_s$, the term of the Schwarzschild metric has a simplified form $1 - r_s/r = 1 - (1 + \rho^2/4r_s^2)^{-1} \cong \rho^2/4r_s^2$. Thus, Eq. (A1) can be written as $ds^2 = -(\rho/2r_s)^2dt^2 + d\rho^2$, which has the same form as the Rindler metric. Moreover, the curvature $1/2r_s$ plays the role of the acceleration α in the Rindler metric.

We here present the details of the derivation of the mapping relation between nonuniform waveguide lattices and space-time with the Rindler metric. According to transformation optics, the evolution of photons in the Rindler metric as Eq. (1) is equivalent to that propagated in such a medium:

$$n_{\text{eff}} = \sqrt{-g_{11}/g_{00}} = 1/\alpha x, \tag{A2}$$

where $g_{00} = -\alpha^2 x^2$, $g_{11} = 1$. And, photons evolve in such a medium and have a corresponding velocity as

$$v = 1/n_{\text{eff}} = \alpha x. \tag{A3}$$

Here nature units have been adopted ($G = c = 1$).

We exploit evanescently coupled photonic waveguide lattices with designed coupling coefficient to achieve the required inhomogeneous effective refractive index. The dynamics of single-photon wave packet in photonic waveguide lattice can be described by a set of coupled discrete Schrödinger equations, which is derived from Schrödinger-type paraxial wave equation by employing the tight-binding approximation:

$$i\partial\varphi_m/\partial z = \beta_0\varphi_m - \kappa_m\varphi_{m-1} - \kappa_{m+1}\varphi_{m+1}, \tag{A4}$$

where φ_m is the complex field amplitude of site m, z is the propagation distance along the waveguides mapping the time variable, β_0 is on-site energy of each waveguide, and parameter κ_m represents the coupling strength between the adjacent sites. Taking coupling coefficients as $\kappa_m = \kappa_{m+1} = \kappa$ and substituting the complex field amplitude with the plane-wave solution $\varphi_m = A\exp(i\beta_x md + i\beta_z z)$, we obtain the dispersion connecting transverse and longitudinal dynamics as

$$\beta_z = \beta_0 - 2\kappa\cos(\beta_x d), \tag{A5}$$

where A is the amplitude of plane wave, β_x (β_z) is transverse and longitudinal wave vector, d is waveguide spacing. After the photons evolve in such a waveguide over distance Δz, each transverse component gains a phase $\Phi = \beta_z(\beta_x)\Delta z$, and the corresponding transverse shift of a wave centered around β_r is $\Delta x = \partial\Phi/\partial\beta_x = \Delta z\,\partial\beta_z/\partial\beta_x$. Owing to that the propagation distance z in the coupled waveguide equation plays the role of the time t in the Schrödinger equation, we define the maximum velocity of wave packets in such a system as

$$v_{\max} = \Delta x/\Delta z = \partial\beta_z/\partial\beta_x = 2\kappa d. \tag{A6}$$

By comparing Eq. (A3) and Eq. (A6) and discretization processing, we obtain the coupling coefficients as

$$\kappa/\kappa_0 = \alpha m/2. \tag{A7}$$

Here we take $x = md$, m is waveguide sites, and κ_0 is the normalized coupling coefficient.

To emulate the Schwarzschild black hole near the event horizon, it requires this condition $\alpha x \ll 1$ in the Rindler metric of Eq. (1). In the respect of waveguide lattices, the distance between waveguides need satisfy this precondition $d \ll 1/m\alpha\kappa_0$. In our computations and plots, the number of waveguides seems a large value and is about $m \approx 100$, which means there is a critical distance between waveguides. Here we take waveguide lattices in silicon on insulator as an example. After assuming $\alpha = 1$, $\kappa_0 \approx 0.001\ \mu\text{m}^{-1}$, $\text{m} \approx 100$, this restriction requires that $d \ll 10\ \mu\text{m}$. Such a distance can be easily achieved by the current (micro)-nanofabrication.

APPENDIX B: THE GREEN FUNCTION OF SUCH NONUNIFORM OPTICAL LATTICES

To obtain the Green function of the emulated accelerated lattice with linear coupling coefficient as waveguide sites, we take the Hamilton operator:

$$H = -\frac{\alpha\kappa_0}{2}\sum_{n=-\infty}^{n=+\infty} n(|n\rangle\langle n+1| + |n+1\rangle\langle n|) + \beta_0\sum_{n=-\infty}^{n=+\infty}|n\rangle\langle n+1|. \tag{B1}$$

Alternatively, one can use a representation in Bloch waves:

$$|k\rangle = \sum_{n=-\infty}^{n=+\infty}|n\rangle\langle n|k\rangle = \sqrt{\frac{1}{2\pi}}\sum_{n=-\infty}^{n=+\infty}|n\rangle e^{ink}, \tag{B2}$$

which satisfies the Bloch condition.

$$\langle n+1|k\rangle = e^{ik}\langle n|k\rangle,$$

with quasimomentum k confined to the Brillouin zone $-\pi \leqslant k \leqslant \pi$. By means of the identities

$$\sum_{n=-\infty}^{n=+\infty} n\langle k'|n+1\rangle\langle n|k\rangle = e^{-ik'}\sum_{n=-\infty}^{n=+\infty} n\langle k'|n\rangle\langle n|k\rangle = e^{-ik'}\frac{1}{2\pi}\sum_{n=-\infty}^{n=+\infty} ne^{in(k-k')} = -e^{-ik'}i\frac{\partial\delta(k'-k)}{\partial k} \tag{B3}$$

$$\sum_{n=-\infty}^{n=+\infty} n\langle k'|n\rangle\langle n+1|k\rangle = e^{ik}\sum_{n=-\infty}^{n=+\infty} n\langle k'|n\rangle\langle n|k\rangle = e^{ik}\frac{1}{2\pi}\sum_{n=-\infty}^{n=+\infty} ne^{in(k-k')} = -e^{ik}i\frac{\partial\delta(k'-k)}{\partial k} \tag{B4}$$

We obtain that the tight-binding Hamiltonian is diagonal:

$$\langle k'|H|k\rangle = \delta(k'-k)H(k), \tag{B5}$$

$$H(k) = -\alpha\kappa_0\cos(k)i\frac{\partial}{\partial k} + \beta_0. \tag{B6}$$

The eigenstates of the Hamiltonian are found by integrating the first-order differential equation

$$-\alpha\kappa_0\cos(k)i\frac{\partial}{\partial k}\Psi(k) + \beta_0\Psi(k) = E\Psi(k), \tag{B7}$$

with the periodic boundary condition $\Psi(k+2\pi) = \Psi(k)$, and $E_m = \beta_0 - \frac{m\alpha\kappa_0}{2}$, one can rewrite Eq. (B7)

$$\Psi_m(k) = \langle k|\Psi_m\rangle = \sqrt{\frac{1}{2\pi}}\exp\left[\frac{2(E_m-\beta_0)\text{arc tan h}\left(\tan\frac{k}{2}\right)}{\alpha\kappa_0}\right] = \sqrt{\frac{1}{2\pi}}\exp\left[-im\text{arc tan h}\left(\tan\frac{k}{2}\right)\right]. \tag{B8}$$

The description in terms of the Wannier states with the Fourier transformation:

$$\Psi_m(n) = \langle n|\Psi_m\rangle = \int_{-\pi}^{\pi} dk\langle n|k\rangle\langle k|\Psi_m\rangle = \frac{1}{2\pi}\int_{-\pi}^{\pi} dke^{i\left[nk-m\cdot\text{arc tan h}\left(\tan\frac{k}{2}\right)\right]} \tag{B9}$$

In the basis of Wannier states one can obtain the propagator as

$$\begin{aligned}
U_{nn'} &= \langle n|U(z)|n'\rangle \\
&= \sum_l \langle n \mid \Psi_l\rangle\, e^{-iE_l z}\langle\Psi_l \mid n'\rangle \\
&= \sum_l \frac{1}{2\pi}\int_{-\pi}^{\pi} dke^{i\left[nk-l\cdot\text{arc tan h}\left(\tan\frac{k}{2}\right)\right]}e^{-i\left(\beta_0-\frac{l\alpha\kappa_0}{2}\right)z}\frac{1}{2\pi}\int_{-\pi}^{\pi} dk'e^{i\left[-n'k'+l\cdot\text{arc tan h}\left(\tan\frac{k'}{2}\right)\right]} \\
&= \sum_l \frac{1}{2\pi}\frac{1}{2\pi}\int_{-\pi}^{\pi}\int_{-\pi}^{\pi} dkdk'e^{i\left[nk-l\cdot\text{arc tan h}\left(\tan\frac{k}{2}\right)-\left(\beta_0-\frac{l\alpha\kappa_0}{2}\right)z-n'k'+l\cdot\text{arc tan h}\left(\tan\frac{k'}{2}\right)\right]} \\
&= \sum_l \frac{1}{2\pi}\frac{1}{2\pi}\int_{-\pi}^{\pi}\int_{-\pi}^{\pi} dkdk'e^{i\left[nk-n'k'-\beta_0 z-l\cdot\text{arc tan h}\left(\tan\frac{k}{2}\right)+l\frac{\alpha\kappa_0 z}{2}+l\cdot\text{arc tan h}\left(\tan\frac{k'}{2}\right)\right]} \\
&= \frac{1}{2\pi}\int_{-\pi}^{\pi}\int_{-\pi}^{\pi} dkdk'e^{i[nk-n'k'-\beta_0 z]}\delta\left(\text{arc tan h}\left(\tan\frac{k}{2}\right) - \text{arc tan h}\left(\tan\frac{k'}{2}\right) - \frac{\alpha\kappa_0 z}{2}\right) \\
&= \frac{1}{2\pi}\int_{-\pi}^{\pi} dk\exp\left\{ink - i2n'\text{arc tan}\left[\tan h\left(\text{arc tan h}\left(\tan\frac{k}{2}\right) - \frac{\alpha\kappa_0 z}{2}\right)\right] - i\beta_0 z\right\},
\end{aligned} \tag{B10}$$

when $\alpha\kappa_0 z/2 \gg 1$, which means photons propagating with large enough distance, one can simplify the Green function as

$$U_{nn'} \approx \frac{1}{2\pi}\int_{-\pi}^{\pi} dk\exp(ink)\exp\left(in'\frac{\pi}{2} - i\beta_0 z\right) = \delta(n)\exp\left(in'\frac{\pi}{2} - i\beta_0 z\right). \tag{B11}$$

APPENDIX C: THE GREEN FUNCTION OF SUCH NONUNIFORM OPTICAL LATTICES

To calculate the entanglement entropy in the accelerated lattice, we exploit the logarithmic negativity to determine the entanglement of such a NOON state ($|\psi\rangle = \frac{1}{2}(a_0^{\dagger 2} + a_1^{\dagger 2})|0\rangle$) evolving in the accelerated lattices. At the initial time, we also depict the entangled pure state $|\psi\rangle = \frac{\sqrt{2}}{2}(|2\rangle_0 + |2\rangle_1)$, which means two indistinguishable photons have the same probability to

concurrently bunching at the event horizon waveguide site ($m = 0$) or its adjacent waveguide site ($m = 1$). After evolving of the path-entangled NOON state in the accelerated lattice, the state can be depicted as

$$|\psi\rangle = \sum_m c_m |2\rangle_m + \sum_{m,n} d_{mn} |1\rangle_m |1\rangle_n, \tag{C1}$$

where c_m represents the probability amplitude of two indistinguishable photons concurrently bunching at m waveguide site, and d_{mn} is the probability amplitude that one photon is locating at m waveguide site and the other photon is locating at n waveguide site. We take the same method as Ref. [51] to numerically calculate the entanglement entropy. In our analysis we trace over all the waveguide sites except for the event horizon waveguide site ($m = 0$) and its adjacent waveguide site ($m = 1$). Among the accelerated lattice, the event horizon waveguide is decoupled from other waveguides due to the coupling between the event horizon waveguide and its adjacent waveguide site is zero. As photons propagating in the event horizon site, photons have no interaction with outside environment waveguide, which implies that photons are in a still state, whereas for photons propagating near the event horizon waveguide site, photons acceleratedly spread into the lattice which is viewed as in an accelerated frame. And the density matrix $\rho = |\varphi\rangle_{AR}\langle\varphi|_{AR}$ (A represents the event horizon waveguide site $m = 0$ and R represents the adjacent waveguide site $m = 1$) can be written as

$$\rho = \begin{array}{c|cccccccccc} & |0_A0_R\rangle & |0_A1_R\rangle & |0_A2_R\rangle & |1_A0_R\rangle & |1_A1_R\rangle & |1_A2_R\rangle & |2_A0_R\rangle & |2_A1_R\rangle & |2_A2_R\rangle \\ \hline \langle 0_A0_R| & \rho_{11} & 0 & 0 & 0 & 0 & 0 & 0 & 0 & 0 \\ \langle 0_A1_R| & 0 & \rho_{22} & 0 & \rho_{24} & 0 & 0 & 0 & 0 & 0 \\ \langle 0_A2_R| & 0 & 0 & \rho_{33} & 0 & 0 & 0 & 0 & 0 & 0 \\ \langle 1_A0_R| & 0 & \rho_{42} & 0 & \rho_{44} & 0 & 0 & 0 & 0 & 0 \\ \langle 1_A1_R| & 0 & 0 & \rho_{53} & 0 & \rho_{55} & 0 & \rho_{57} & 0 & 0 \\ \langle 1_A2_R| & 0 & 0 & 0 & 0 & 0 & 0 & 0 & 0 & 0 \\ \langle 2_A0_R| & 0 & 0 & \rho_{73} & 0 & 0 & 0 & \rho_{77} & 0 & 0 \\ \langle 2_A1_R| & 0 & 0 & 0 & 0 & 0 & 0 & 0 & 0 & 0 \\ \langle 2_A2_R| & 0 & 0 & 0 & 0 & 0 & 0 & 0 & 0 & 0 \end{array}. \tag{C2}$$

By calculating the eigenvalue of the partial transpose of density matrix ρ, we sum over all the negative values and obtained the total number N^T. The entanglement entropy is defined as

$$E_s = \log_2(1 + 2|N^T|). \tag{C3}$$

[1] B. P. Abbott *et al.*, Phys. Rev. Lett. **116**, 061102 (2016).
[2] B. P. Abbott *et al.*, Phys. Rev. Lett. **119**, 161101 (2017).
[3] K. Akiyama *et al.*, Astrophys. J. **875**, L1 (2019).
[4] S. W. Hawking, Nature (London) **248**, 30 (1974).
[5] R. Penrose and R. M. Floyd, Nat. Phys. Sci. **229**, 177 (1971).
[6] A. Aspuru-Guzik and P. Walther, Nat. Phys. **8**, 285 (2012).
[7] R. Blatt and C. F. Roos, Nat. Phys. **8**, 277 (2012).
[8] I. Bloch, J. Dalibard, and S. Nascimbene, Nat. Phys. **8**, 267 (2012).
[9] W. G. Unruh, Phys. Rev. D **14**, 870 (1976).
[10] J. Hu, L. Feng, Z. Zhang, and C. Chin, Nat. Phys. **15**, 785 (2019).
[11] J. R. M. de Nova, K. Golubkov, V. I. Kolobov, and J. Steinhauer, Nature (London) **569**, 688 (2019).
[12] B. Horstmann, B. Reznik, S. Fagnocchi, and J. I. Cirac, Phys. Rev. Lett. **104**, 250403 (2010).
[13] S. Giovanazzi, Phys. Rev. Lett. **94**, 061302 (2005).
[14] P. D. Nation, M. P. Blencowe, A. J. Rimberg, and E. Buks, Phys. Rev. Lett. **103**, 087004 (2009).
[15] T. G. Philbin, C. Kuklewicz, S. Robertson, S. Hill, F. Konig, and U. Leonhardt, Science **319**, 1367 (2008).
[16] F. Belgiorno, S. L. Cacciatori, M. Clerici, V. Gorini, G. Ortenzi, L. Rizzi, E. Rubino, V. G. Sala, and D. Faccio, Phys. Rev. Lett. **105**, 203901 (2010).
[17] J. Drori, Y. Rosenberg, D. Bermudez, Y. Silberberg, and U. Leonhardt, Phys. Rev. Lett. **122**, 010404 (2019).
[18] J. B. Pendry, A. J. Holden, D. J. Robbins, and W. J. Stewart, IEEE Trans. Microwave Theory Tech. **47**, 2075 (1999).
[19] R. A. Shelby, D. R. Smith, and S. Schultz, Science **292**, 77 (2001).
[20] J. B. Pendry, D. Schurig, and D. R. Smith, Science **312**, 1780 (2006).
[21] U. Leonhardt, Science **312**, 1777 (2006).
[22] H. Chen, C. T. Chan, and P. Sheng, Nat. Mater. **9**, 387 (2010).
[23] D. A. Genov, S. Zhang, and X. Zhang, Nat. Phys. **5**, 687 (2009).
[24] E. E. Narimanov and A. V. Kildishev, Appl. Phys. Lett. **95**, 041106 (2009).
[25] Q. Cheng, T. J. Cui, W. X. Jiang, and B. G. Cai, New J. Phys. **12**, 063006 (2010).
[26] H. Chen, R.-X. Miao, and M. Li, Opt. Express **18**, 15183 (2010).
[27] C. Sheng, H. Liu, Y. Wang, S. N. Zhu, and D. A. Genov, Nat. Photonics **7**, 902 (2013).
[28] T. G. Mackay and A. Lakhtakia, Phys. Lett. A **374**, 2305 (2010).
[29] C. Sheng, H. Liu, H. Chen, and S. Zhu, Nat. Commun. **9**, 4271 (2018).

[30] C. Sheng, R. Bekenstein, H. Liu, S. Zhu, and M. Segev, Nat. Commun. **7**, 10747 (2016).
[31] A. Greenleaf, Y. Kurylev, M. Lassas, and G. Uhlmann, Phys. Rev. Lett. **99**, 183901 (2007).
[32] J. Zhu, Y. Liu, Z. Liang, T. Chen, and J. Li, Phys. Rev. Lett. **121**, 234301 (2018).
[33] R. Q. He, G. H. Lang, S. N. Zhu, and H. Liu, Phys. Rev. Research **2**, 013237 (2020).
[34] I. I. Smolyaninov and Y.-J. Hung, J. Opt. Soc. Am. B **28**, 1591 (2011).
[35] V. Ginis, P. Tassin, B. Craps, and I. Veretennicoff, Opt. Express **18**, 5350 (2010).
[36] Y. Wang *et al.*, Natl. Sci. Rev. **7**, 1476 (2020).
[37] C. Koke, C. Noh, and D. G. Angelakis, Ann. Phys. **374**, 162 (2016).
[38] A. J. Kollar, M. Fitzpatrick, and A. A. Houck, Nature (London) **571**, 45 (2019).
[39] I. Boettcher, P. Bienias, R. Belyansky, A. J. Kollar, and A. V. Gorshkov, Phys. Rev. A **102**, 032208 (2020).
[40] Y. Bromberg, Y. Lahini, R. Morandotti, and Y. Silberberg, Phys. Rev. Lett. **102**, 253904 (2009).
[41] Y. Bromberg, Y. Lahini, and Y. Silberberg, Phys. Rev. Lett. **105**, 263604 (2010).
[42] A. S. Solntsev, A. A. Sukhorukov, D. N. Neshev, and Y. S. Kivshar, Phys. Rev. Lett. **108**, 023601 (2012).
[43] K. Poulios *et al.*, Phys. Rev. Lett. **112**, 143604 (2014).
[44] A. S. Solntsev, F. Setzpfandt, A. S. Clark, C. W. Wu, M. J. Collins, C. Xiong, A. Schreiber, F. Katzschmann, F. Eilenberger, R. Schiek, W. Sohler, A. Mitchell, C. Silberhorn, B. J. Eggleton, T. Pertsch, A. A. Sukhorukov, D. N Neshev, and Y. S. Kivshar, Phys. Rev. X **4**, 031007 (2014).
[45] H. Tang *et al.*, Nat. Photonics **12**, 754 (2018).
[46] H. Tang *et al.*, Sci. Adv. **4**, eaat3174 (2018).
[47] M. Christandl, N. Datta, A. Ekert, and A. J. Landahl, Phys. Rev. Lett. **92**, 187902 (2004).
[48] M. B. Plenio and S. F. Huelga, New J. Phys. **10**, 113019 (2008).
[49] M. Fathi and R. T. Thompson, Phys. Rev. D **93**, 124026 (2016).
[50] L. C. B. Crispino, A. Higuchi, and G. E. A. Matsas, Rev. Mod. Phys. **80**, 787 (2008).
[51] I. Fuentes-Schuller and R. B. Mann, Phys. Rev. Lett. **95**, 120404 (2005).